

Prediction of the Stress Wave Amplification Factor of a Spherical Blast Source Using Numerical Simulations

Jawad Ur Rehman

Department of Civil and Environmental Engineering
Hanyang University
Seoul, South Korea
jawad640@hanynag.ac.kr

Tuan-Anh Nguyen

Department of Civil Engineering
Vinh University
Vinh, Vietnam
anhhandico52@gmail.com

Trong-Kien Nguyen

Department of Civil Engineering
Vinh University
Vinh, Vietnam
nguyentrongkien82@gmail.com

Can-Ngon Nguyen

Department of Civil Engineering
Vinh University
Vinh, Vietnam
ngon_nguyencan@yahoo.com

Trong-Cuong Vo

Department of Civil Engineering
Vinh University
Vinh, Vietnam
cuongvqc@gmail.com

Van-Quang Nguyen

Department of Civil Engineering
Vinh University
Vinh, Vietnam
nguyenvanquang240484@gmail.com

Received: 2 August 2022 | Revised: 25 August 2022 | Accepted: 27 August 2022

Abstract—A typical blast wave attenuation curve presents a relationship between Peak Particle Velocity (PPV) at the surface of a geologic profile and distance. As the stress wave is amplified at the free-field boundary, the attenuation curve at the surface is always larger than the within media profile curve. Measurements are made at the rock's surface and test blasts are always conducted to ensure the safety of underground existing structures. In order to design underground blasting, the recorded PPVs are then reduced by a factor of 2. In this paper, particle velocity amplification was studied by using numerical simulation, and the difference between PPV at the surface and within media profiles is quantified. The amplification factor depends upon source depth, incidence angle, and Poisson's ratio of the media. It is calculated as the ratio of the magnitude of PPV at the surface of the media to the within media profile. According to the parametric study, the amplification factor for a uniform medium increases with increasing source depth, while the amplification factor decreases with increasing Poisson's ratio. Considering a three-layer model with a source depth of 30m, the amplification factor is high for low incident angles and low for higher incident angles. The range varies between 1.5 to 2.1.

Keywords—free surface; numerical simulation; underground blasting; wave amplification; wave attenuation

I. INTRODUCTION

Blasting is one of the most extensively utilized methods for extracting rock in mining and construction operations and the most cost-effective excavation method [1]. The appropriate design of blasts and the management and prediction of blast consequences importance is increasing as the magnitude of these operations grows [2, 3]. The majority of the explosive energy is utilized in the crushing and fracturing of the rock mass. When blasting energy is transferred to the rock mass, it might cause damage to the surrounding rock in the form of undesired fractures. Many researchers have contributed to the development of the blast vibration safety criterion, and several criteria or prediction models have been proposed to assess the structural stability of diverse constructions [4, 5]. Peak Particle Velocity (PPV) is the most extensively used indicator for evaluating blast-induced damage. PPVs are widely assumed to be determinable in empirical models based on the maximum charge per delay, distance from the blasting source, and site coefficients. The scaled distance concept proposed by the United States Bureau of Mines (USBM) [6] is the most acceptable vibration prediction equation. It takes into account the quantity of explosive energy in shock and seismic waves, as well as distance effects. Test blasts are usually conducted to record surface PPVs, and an attenuation curve is then

developed by conducting regression analysis. The Scaled Distance (SD) is calculated by taking the distance between the source and measurement locations and dividing it by the maximum charge per delay:

$$SD = \frac{R}{\sqrt{W}} \quad (1)$$

where R is the distance between the charge and monitoring station and W is the maximum charge weight per delay.

The USBM predictor equation for the estimation of the peak particle velocity is:

$$PPV = K(SD)^n \quad (2)$$

where K and n are the site and geological constant factors respectively.

The ground transmission factor, or constant K , is influenced by the confinement of the charge, and the local geology. Higher values of K denote either well-coupled explosives or a mass of rock that is relatively large and fracture-free. The quality of the rock mass affects the constant n , which indicates the impact of attenuation with distance. Lower values of n indicate more competent rock mass with less fracturing, whereas higher values of n indicate poorer quality rock mass that attenuates vibration energy more quickly and within a shorter distance from the charge.

Test blasts are usually conducted to record surface PPVs, and an attenuation curve is then developed by regression analysis. Artificial Intelligence (AI) techniques like Artificial Neural Networks (ANNs) and Particle Swarm Optimization (PSO) have been utilized in mining and civil engineering during the last few years to forecast the PPV based on total charge, distance, maximum charge per delay, frequency, and blasting parameters [7, 8]. Previously, the wave amplification effect studies mainly focused on earthquakes [9-14] and the amplification effect for the blast source has not been studied extensively. This paper uses numerical simulations to study the amplification factors using a spherical blast source.

II. NUMERICAL MODELING

In the present study, numerical analysis is carried out using FLAC 2D version 7.0 [15]. An axisymmetric model with a spherical blast source and a quad mesh with a mesh size of 0.05m is used. The blast-induced fracture zone is described as a spherical cavity with a radius of 0.5m. The half-space was modeled as an elastic material. The computational model and boundary conditions are shown in Figure 1. The reflected wave created at the upper boundary travels to the side wall and the lower end as it propagates in the radial direction with vertical and horizontal velocity components. Therefore, viscous dampers are installed in two directions, at the side wall and at the bottom to absorb the impact of vibrations, as suggested in [16]. The modelling strategy used in this paper is as follows: first, a geometric model of the rock mass is created and a behavioural model and material properties are applied. Then, a mesh is generated, boundary conditions and viscous boundaries are applied, and finally, a blast load is applied.

The explosion depths employed were 10, 20, and 30m. The computational domain has a 70m lateral dimension. The blast

load was applied to the cavity surface in the normal direction as a pressure-time history.

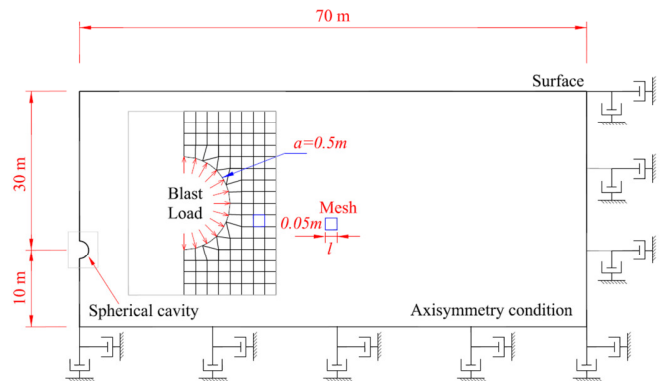


Fig. 1. The computational model.

To verify the numerical model, the results of the dynamic analysis for the undamped case are compared to the closed-form solution in [17]. To solve the spherical charge blasting vibration problem, the authors in [17] simplified the cavity-blasting pressure. The solution showed that the spherical blasting generates only P waves, and an elastic velocity equation for the spherical blasting vibration was later obtained as follows:

$$V(R, \bar{\tau}) = -\frac{a}{R} f(\bar{\tau}) - \left(\frac{a}{R}\right)^2 q(\bar{\tau}) \quad (3)$$

where V is the velocity induced by the blast source, a is the source cavity, R is the distance from the measured point to the charge centre, $f(\tau)$, $q(\tau)$ are time history functions of the wave at R , and τ is the dimensionless time.

$$f(\bar{\tau}) = c \frac{\partial^2 \phi_1}{\partial \bar{\tau}^2}, q(\bar{\tau}) = c \frac{\partial \phi_1}{\partial \bar{\tau}} \quad (4)$$

where c is the wave velocity and ϕ_1 is the displacement potential function:

$$\phi_1 = \frac{-pc}{\rho_d b_{2d}} \left\{ \left(\bar{\tau} - 2 \frac{b_{1d}}{b_{2d}} \right) e^{-\alpha_c \bar{\tau}} + e^{-\alpha_d \bar{\tau}} \left[\frac{b_{1d}}{\sqrt{b_{2d} \omega_d}} \cos(\omega_d \bar{\tau} - \theta) - \frac{1}{\sqrt{b_{2d}}} \sin(\omega_d \bar{\tau} - \theta) \right] \right\}$$

where:

$$p_c = \frac{P_0}{E} \left(\frac{a}{c}\right)^n, \bar{\tau} = \left(t - \frac{R-a}{c}\right) \frac{c}{a}, \omega_d = \frac{(1-2\nu)^{1/2}}{(1-\nu)}, \alpha_d = \frac{(1-2\nu)}{(1-\nu)}, \alpha_c = \frac{a}{c} \alpha, b_{1d} = \frac{a}{c} (\alpha_0 - \alpha), b_{2d} = \left(\frac{a}{c}\right)^2 (\omega_0^2 + (\alpha_0 - \alpha)^2), \theta = \frac{b_{1d}}{\omega_d}.$$

Time-varying blast pressure is applied to the wall of an equivalent cavity using the following formulation [17]:

$$P(t) = P_0 t^n e^{-\beta t} \quad (4)$$

where $P(t)$ and P_0 denote time-varying blast pressure and initial detonation pressure respectively, t represents time, n is an integer, and β denotes decay of the pressure pulse. Figure 2

shows a blast pressure profile calculated using $(P(t) = P_0 t^n e^{-\beta t})$.

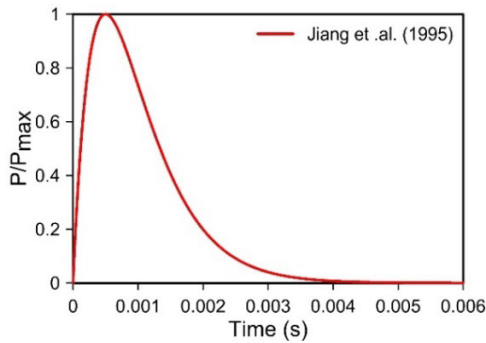


Fig. 2. Pressure time history applied to the wall of an equivalent cavity.

The velocity-time history estimated from the numerical simulation and the equation from [17] for the undamped medium is shown in Figure 3. The shear wave was fixed to 2309m/s, with a Poisson ratio of 0.25, whereas unit weight was set at 24.5kN/m³. The selected loading pressure was 1GPa. n and β were set to 1 and 2000 respectively. The blast equivalent cavity was assumed as 0.5m. It is shown that the numerical model correctly predicts the wave attenuation, providing results that are almost identical to the analytical solution. A parametric study is conducted to study the influence of effective parameters on wave amplification at the surface. These parameters include source depth, angle of incidence, and Poisson's ratio. First, a homogeneous rock mass is modeled and then layered model with weathered rock at the surface, followed by soft rock, and then hard rock mass is considered.

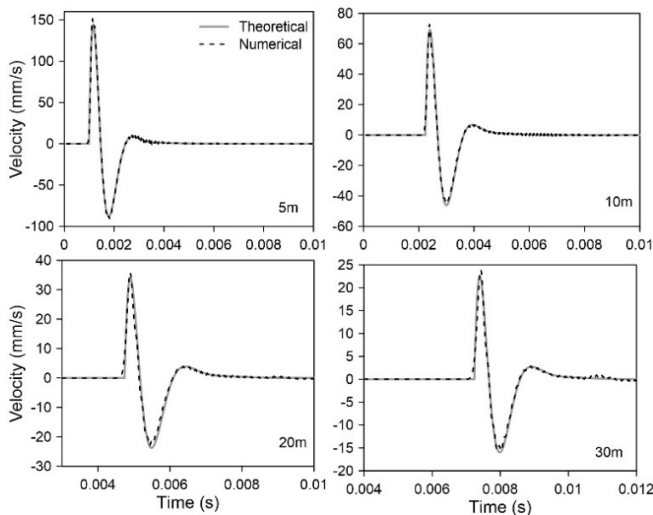


Fig. 3. Comparison of the numerical simulation with a closed-form solution.

III. RESULTS AND DISCUSSION

Blast-induced vibrations are usually recorded in the form of PPV at the surfaces. Surface vibrations are always higher than within profiles [18]. Table I shows the mechanical properties of the rock mass [19]. The attenuation of PPV for surface and

within profiles for the depth of 30m with Poisson's ratio of 0.25 is shown in Figure 4. The calculated PPV at the surface is almost two times the one within profiles.

TABLE I. MECHANICAL PROPERTIES OF THE ROCK MASS [19]

Rock type	Shear velocity (m/s)	Unit weight (kN/m ³)	Poisson ratio
Hard Rock	2500	25	0.25
	2000		
	1500		
Soft Rock	1200	23	0.27
	1000		
	800		
Weathered Rock	650	21	0.3
	500		
	150		

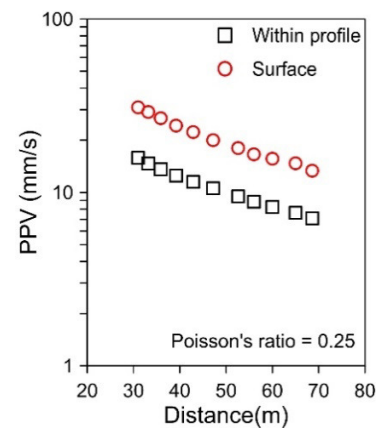


Fig. 4. Comparison of PPV within profile and surface for homogenous media.

To study the amplification factor in detail, three source depths of 10, 20, and 30m from the surface are considered. Three Poisson's ratios of 0.20, 0.25, and 0.30 are selected. For uniform homogeneous rock mass, Figure 5(a) shows the results of Poisson's ratio of 0.20, for the three depths. The amplification factor at high angles is 1.8, whereas at lower angles it increases up to 2. A source at greater depth shows an amplification factor near to 2 at 10° to 50°. For Poisson's ratio of 0.25, at high angles the amplification factor in Figure 5(b) is 1.7 and at lower angles it is 2. The amplification factor for Poisson's ratio of 0.30 in Figure 5(c) is 1.5 at higher angles and 1.9 at lower angles. Low Poisson's ratio has amplification from near 1.8 to 2.1, whereas higher Poisson's ratio shows less amplification factor and gradually increases for lower angles up to 1.9.

Until now, the rock mass was considered homogenous, however, in the real field, it is inhomogeneous. For this purpose, a three-layer model is developed: near the surface the rock mass consists of soft rock, followed by weathered rock, and the lower most part consists of hard rock. Figure 6 shows the computational model for inhomogeneous rock mass. The attenuated PPV at 30m depth is shown in Figure 7. The amplification factor at smaller distances, i.e. at lower incident angles, is more than 2, whereas at greater distances, i.e. at higher incident angles, the amplification factor is 1.5. To further get a clear view, Figure 8 shows the amplification factor

at 30m depth, which shows high amplification factor for low incident angles. The amplification factor decreases for higher angles.

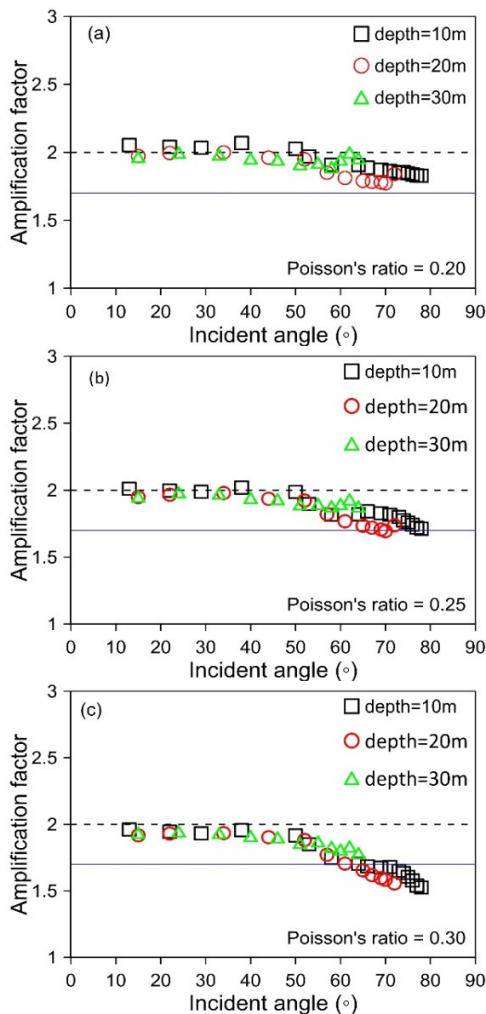


Fig. 5. Amplification factor for homogeneous rock: (a) $\nu = 0.20$, (b) $\nu = 0.25$, (c) $\nu = 0.30$.



Fig. 6. A computational model for inhomogeneous rock mass.

The results show that the inhomogeneity of rock mass plays a vital role in wave amplification. Amplification factors for different sites will be different based upon rock mass strata. Many studies [20] assume an amplification factor of 2 for homogenous rock mass using a spherical blast source. A numerical simulation is suggested for finding amplification

factors for the specific site. This study is limited to spherical blast sources. In the field, cylindrical blast sources are utilized. Future research will include a complete parametric investigation employing a cylindrical blast source.

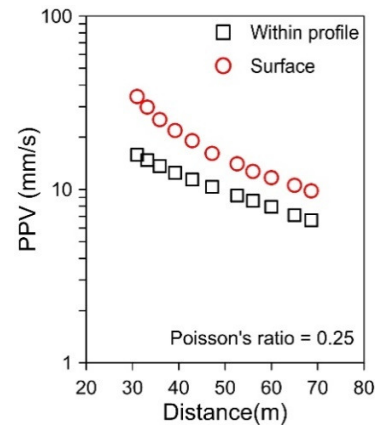


Fig. 7. Comparison of PPV of within profile and surface for inhomogeneous rock mass.

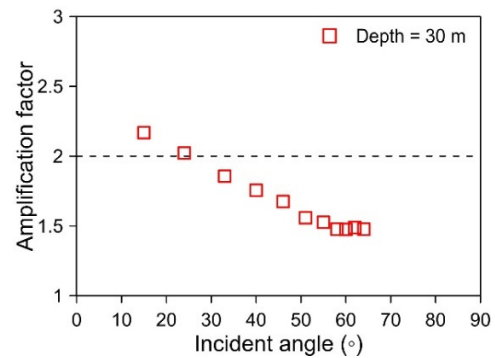


Fig. 8. Amplification factor for inhomogeneous rock mass

IV. CONCLUSIONS

This paper presented a numerical analysis-based amplification factor for a spherical blast source. The velocity amplification factor is defined as the ratio of wave amplitude at the free field boundary to the incident wave amplitude. Poisson's ratio, source depth, angle of incidence, and geological characteristic of a specific site are the main factors that affected the velocity amplification. The results show that the amplification factor varies between 1.5 to 2.1.

As a consequence, velocity amplification phenomena should be taken into account while assessing underground damage. It is recommended to utilize numerical analysis to predict site-specific amplification factor, which can improve design procedures and help engineers predict the inner profile attenuation curves for controlling damage to the surrounding rock mass.

REFERENCES

[1] I. A. Onederra, J. K. Furtney, E. Sellers, and S. Iverson, "Modelling blast induced damage from a fully coupled explosive charge," *International Journal of Rock Mechanics and Mining Sciences*, vol. 58, pp. 73–84, Feb. 2013, <https://doi.org/10.1016/j.ijrmm.2012.10.004>.

- [2] L. Malmgren, D. Saiang, J. Töyrä, and A. Bodare, "The excavation disturbed zone (EDZ) at Kiirunavaara mine, Sweden—by seismic measurements," *Journal of Applied Geophysics*, vol. 61, no. 1, pp. 1–15, Jan. 2007, <https://doi.org/10.1016/j.jappgeo.2006.04.004>.
- [3] D. Saiang and E. Nordlund, "Numerical Analyses of the Influence of Blast-Induced Damaged Rock Around Shallow Tunnels in Brittle Rock," *Rock Mechanics and Rock Engineering*, vol. 42, no. 3, pp. 421–448, Jun. 2009, <https://doi.org/10.1007/s00603-008-0013-1>.
- [4] J.-H. Shin, H.-G. Moon, and S.-E. Chae, "Effect of blast-induced vibration on existing tunnels in soft rocks," *Tunnelling and Underground Space Technology*, vol. 26, no. 1, pp. 51–61, Jan. 2011, <https://doi.org/10.1016/j.tust.2010.05.004>.
- [5] P. Pal Roy, "Vibration control in an opencast mine based on improved blast vibration predictors," *Mining Science and Technology*, vol. 12, no. 2, pp. 157–165, Mar. 1991, [https://doi.org/10.1016/0167-9031\(91\)91642-U](https://doi.org/10.1016/0167-9031(91)91642-U).
- [6] W. I. Duvall and D. E. Fogelson, *RI 5968 Review of Criteria for Estimating Damage to Residences from Blasting Vibrations? Summary and Conclusions*. Washington DC, USA: United States Department of the Interior, 1962.
- [7] D. J. Armaghani, M. Hajihassani, E. T. Mohamad, A. Marto, and S. A. Noorani, "Blasting-induced flyrock and ground vibration prediction through an expert artificial neural network based on particle swarm optimization," *Arabian Journal of Geosciences*, vol. 7, no. 12, pp. 5383–5396, Dec. 2014, <https://doi.org/10.1007/s12517-013-1174-0>.
- [8] D. J. Armaghani, E. Momeni, S. V. A. N. K. Abad, and M. Khandelwal, "Feasibility of ANFIS model for prediction of ground vibrations resulting from quarry blasting," *Environmental Earth Sciences*, vol. 74, no. 4, pp. 2845–2860, Aug. 2015, <https://doi.org/10.1007/s12665-015-4305-y>.
- [9] M. Aaqib, D. Park, M. B. Adeel, Y. M. A. Hashash, and O. Ilhan, "Simulation-based site amplification model for shallow bedrock sites in Korea," *Earthquake Spectra*, vol. 37, no. 3, pp. 1900–1930, Aug. 2021, <https://doi.org/10.1177/8755293020981984>.
- [10] M. Aaqib, D. Park, Y.-G. Lee, and U. Pervaiz, "Development of Site Classification System and Seismic Site Coefficients for Korea," *Journal of Earthquake Engineering*, Oct. 2021, <https://doi.org/10.1080/13632469.2021.1990164>.
- [11] Y. Lee, H.-S. Kim, M. I. Khalid, Y. Lee, and D. Park, "Effect of Nonlinear Soil Model on Seismic Response of Slopes Composed of Granular Soil," *Advances in Civil Engineering*, vol. 2020, Nov. 2020, Art. no. e8890247, <https://doi.org/10.1155/2020/8890247>.
- [12] T. Nagao, "Seismic Amplification by Deep Subsurface and Proposal of a New Proxy," *Engineering, Technology & Applied Science Research*, vol. 10, no. 1, pp. 5157–5163, Feb. 2020, <https://doi.org/10.48084/etasr.3276>.
- [13] T. Nagao, "Maximum Credible Earthquake Ground Motions with Focus on Site Amplification due to Deep Subsurface," *Engineering, Technology & Applied Science Research*, vol. 11, no. 2, pp. 6873–6881, Apr. 2021, <https://doi.org/10.48084/etasr.3991>.
- [14] T. Nagao, "Variation Evaluation of Path Characteristic and Site Amplification Factor of Earthquake Ground Motion at Four Sites in Central Japan," *Engineering, Technology & Applied Science Research*, vol. 11, no. 5, pp. 7658–7664, Oct. 2021, <https://doi.org/10.48084/etasr.4405>.
- [15] "FLAC (Fast Lagrangian Analysis of Continua) Version 220," Itasca Consulting Group, Inc., Minneapolis, MN (USA) Nuclear Regulatory Commission, Washington, DC (USA), Report NUREG/CR-5430-VOL.3, 1989.
- [16] J. Lysmer and R. L. Kuhlemeyer, "Finite Dynamic Model for Infinite Media," *Journal of the Engineering Mechanics Division*, vol. 95, no. 4, pp. 859–877, Aug. 1969, <https://doi.org/10.1061/JMCEA3.0001144>.
- [17] J. Jiang, D. P. Blair, and G. R. Baird, "Dynamic response of an elastic and viscoelastic full-space to a spherical source," *International Journal for Numerical and Analytical Methods in Geomechanics*, vol. 19, no. 3, pp. 181–193, 1995, <https://doi.org/10.1002/nag.1610190303>.
- [18] J.-K. Ahn and D. Park, "Prediction of Near-Field Wave Attenuation Due to a Spherical Blast Source," *Rock Mechanics and Rock Engineering*, vol. 50, no. 11, pp. 3085–3099, Nov. 2017, <https://doi.org/10.1007/s00603-017-1274-3>.
- [19] J.-K. Ahn, D. Park, and J.-K. Yoo, "Estimation of damping ratio of rock mass for numerical simulation of blast induced vibration propagation," *Japanese Geotechnical Society Special Publication*, vol. 2, no. 45, pp. 1589–1592, 2016, <https://doi.org/10.3208/jgssp.KOR-34>.
- [20] P. Zhang, E. Nordlund, G. Swan, and C. Yi, "Velocity Amplification of Seismic Waves Through Parallel Fractures Near a Free Surface in Fractured Rock: A Theoretical Study," *Rock Mechanics and Rock Engineering*, vol. 52, no. 1, pp. 199–213, Jan. 2019, <https://doi.org/10.1007/s00603-018-1589-8>.